



## Article

# Differential Cytotoxicity, Inflammatory Responses, and Aging Effects of Human Skin Cells in Response to Fine Dust Exposure

Tae Eun Kim <sup>†</sup> , Jun Woo Lim <sup>†</sup>, Jae Hyun Jeong <sup>\*†</sup>  and Hee Wook Ryu <sup>\*</sup>

Department of Chemical Engineering, Soongsil University, 369, Sangdo-ro, Dongjak-gu, Seoul 06978, Republic of Korea; taeat@soongsil.ac.kr (T.E.K.); ljw9424@naver.com (J.W.L.)

<sup>\*</sup> Correspondence: nfejjh@ssu.ac.kr (J.H.J.); hwryu@ssu.ac.kr (H.W.R.)

<sup>†</sup> These authors contributed equally to this work.

**Abstract:** Airborne fine dust pollution poses a significant threat to both respiratory and skin health, yet the skin's physiological response to such exposure has been underexplored. This study investigates the impact of fine dust on skin cells, focusing on their metabolic activity, inflammatory responses, and aging-related changes. We found that exposure to fine dust model compounds led to dose-dependent cytotoxicity, with PM<sub>2.5</sub>-Ions exhibiting higher toxicity compared to PM<sub>10</sub>-PAHs. Human epithelial keratinocytes (HEK<sub>n</sub>) showed heightened sensitivity to fine dust, marked by increased inflammation, particularly with elevated IL-8 expression in response to PM<sub>2.5</sub>-Ions. Additionally, fine dust exposure resulted in reduced cell density, slower proliferation, and decreased migration, notably at higher concentrations of PM<sub>2.5</sub>-Ions. These changes are indicative of accelerated aging processes, including compromised cell function and structural integrity. Live cell imaging and correlation analyses highlighted significant links between metabolic activity, cell morphology, and IL-8 secretion. These findings provide critical insights into the differential impacts of fine dust components on skin cells, emphasizing the potential acceleration of aging processes and underscoring the need for further research on cellular responses to environmental stress and the development of protective measures against urban fine dust exposure. Overall, this study, which contributes to addressing the skin health risks posed by air pollutants, could be actively used in environmental science, dermatology, and public health.

**Keywords:** fine dust; PM<sub>2.5</sub>; PM<sub>10</sub>; cytotoxicity; inflammation; human dermal fibroblasts; human epidermal keratinocytes



**Citation:** Kim, T.E.; Lim, J.W.; Jeong, J.H.; Ryu, H.W. Differential Cytotoxicity, Inflammatory Responses, and Aging Effects of Human Skin Cells in Response to Fine Dust Exposure. *Environments* **2024**, *11*, 259. <https://doi.org/10.3390/environments11110259>

Academic Editors: Sripriya Nannu Shankar, Tara Sabo-Attwood, Jana S. Kesavan and Sanghee Han

Received: 15 September 2024  
Revised: 3 November 2024  
Accepted: 16 November 2024  
Published: 19 November 2024



**Copyright:** © 2024 by the authors. Licensee MDPI, Basel, Switzerland. This article is an open access article distributed under the terms and conditions of the Creative Commons Attribution (CC BY) license (<https://creativecommons.org/licenses/by/4.0/>).

## 1. Introduction

Airborne fine dust pollution is on the rise, presenting a rapidly increasing and significant threat to both the environment and human health [1]. Fine dust particles suspended in the atmosphere not only affect respiratory health but also make direct contact with the skin, rendering the skin one of the primary organs exposed to external pollutants [2]. While research on the health effects of fine dust has mainly concentrated on its impacts on pulmonary [3] and cardiovascular systems [4], the consequences for skin health have often been overlooked. Nonetheless, the skin is highly responsive to environmental exposures and serves as the body's first line of defense [5]. Therefore, understanding the intricate interplay between fine dust and skin health has become a matter of paramount importance [6].

Fine dust particles, specifically PM<sub>2.5</sub> (fine dust with diameters below 2.5 μm) and PM<sub>10</sub> (below 10 μm), encompass a complex mixture of organic and inorganic compounds [7], including polycyclic aromatic hydrocarbons (PAHs), trace elements, and ions [8]. PAHs are classified as carcinogens and are known to induce inflammation and cancer development [9,10]. Exposure to trace elements affects cognitive and mental disorders, while ions are associated with an increased risk of cardiovascular diseases [11]. Despite the

well-documented adverse effects of fine dust on various organ systems [12], the impact on skin health remains relatively unexplored. The skin is the largest organ of the human body and serves as a protective barrier against the external environment. It consists mainly of the epidermis and dermis, and understanding how the cells in each layer respond to and recover from the infiltration of fine dust is essential. Therefore, epidermal keratinocytes, representing the epidermal layer, and dermal fibroblasts, representing the dermal layer, were selected to analyze the physiological effects. Skin cells, comprising epidermal keratinocytes and dermal fibroblasts, directly encounter fine dust, triggering responses such as oxidative stress, inflammation, and DNA damage [2,13].

Therefore, this study aims to bridge the gap in our understanding of the physiological responses of skin cells to fine dust exposure. Utilizing a fine dust model compound capable of simulating diverse environmental conditions, we conducted a comprehensive analysis of the metabolic activity and behavior of skin cells. Exposure to model fine dust compounds induces dose-dependent cytotoxicity, with PM<sub>2.5</sub>-ions exhibiting higher toxicity compared to PM<sub>10</sub>-PAHs. Human epidermal keratinocytes (HEK<sub>n</sub>) showed increased sensitivity to fine dust, leading to heightened inflammation, particularly marked by increased IL-8 expression in response to PM<sub>2.5</sub>-ions. Moreover, exposure to fine dust resulted in reduced cell density, delayed proliferation, and decreased migration, with these effects being more pronounced at higher concentrations of PM<sub>2.5</sub>-ions. These changes indicate an accelerated aging process, characterized by impaired cellular function and structural integrity. Live cell imaging and correlation analysis highlighted significant associations between metabolic activity, cell morphology, and IL-8 secretion. Interestingly, our investigation includes a simulated mixed model emulating Seoul's atmospheric fine dust composition, which showcases reduced cellular toxicity compared to individual components. This finding underscores the complex interactions inherent in real-world fine dust and highlights the importance of considering the holistic impact of fine dust pollution on skin health.

## 2. Experimental Methods

### 2.1. Preparation and Treatment of Fine Dusts

Fine dusts were classified based on size into fine dust with diameters below 2.5 µm (PM<sub>2.5</sub>) and below 10 µm (PM<sub>10</sub>). To evaluate the physiological effects of fine dust on skin cells, certified reference materials (CRMs) with various particle sizes and chemical properties were purchased and used. Three types of CRMs were used in this study: CRM-PM<sub>2.5</sub>-Ions (ERM-CZ110, Sigma-Aldrich, MO, USA), CRM-PM<sub>10</sub>-PAHs (ERM-CZ100, Sigma-Aldrich, MO, USA), and CRM-PM<sub>10</sub>-Trace (ERM-CZ1200, Sigma-Aldrich, MO, USA). The three types of CRMs consist of various chemical and physical compounds, including polynuclear aromatic hydrocarbons (PAHs), trace elements, ions, organic compounds, transition metals, and biological components. CRM-PMs were sterilized under UV light for 30 min, dispersed in 1× phosphate-buffered saline (PBS, Biowest, Nuaille, France) at a concentration of 500 µg/mL, and sonicated for one hour. Final concentrations of 2, 10, 50, and 100 µg/mL were prepared by diluting the CRM-PM stock solutions in proliferation media. The composition of each CRM-PM component is detailed in Tables S1–S3.

### 2.2. Cell Culture of Human Skin Cells

In this study, epidermal keratinocytes and dermal fibroblasts were selected to analyze the physiological effects of fine dust on skin cells within the epidermis and dermis of the skin. Human dermal fibroblasts, neonatal (HDFn cells in passages 3 to 5, Gibco, Grand Island, NY, USA), were cultured in a 75-cm<sup>2</sup> cell culture flask using Human Fibroblast Expansion Basal Medium (Gibco, Grand Island, NY, USA) supplemented with Low Serum Growth Supplement (LSGS, Gibco, Grand Island, NY, USA) and 1% penicillin-streptomycin (P/S, 100x, Biowest, Nuaille, France). Human epidermal keratinocytes (HEK<sub>n</sub> cells in passages 1 to 3, Gibco, Grand Island, NY, USA) were cultured in a 75-cm<sup>2</sup> cell culture flask using EpiLife™ Medium, with 60 µM calcium (Gibco, Grand Island, NY, USA) supplemented with Human Keratinocyte Growth Supplement (HKGS, Gibco, Grand Island, NY,

USA) and 1% penicillin-streptomycin (P/S, 100x, Biowest, Watertown, MA, USA). Cells were maintained in a 5% CO<sub>2</sub>, 37 °C environment, with a media change every two days. When reaching 80% confluence, cells were detached from the flask using 0.25% Trypsin (Biowest, France) for further experimentation. Throughout each experimental process, cells were observed using an optical microscope (Nikon Eclipse TS100, Nikon Corporation, Tokyo, Japan).

### 2.3. Cell Viability Assay

To assess the toxic impact of fine dust on skin cells, cell viability was measured using the MTT assay with optical density (OD) readings. Viable cells can reduce MTT to formazan compounds, and cell viability can be calculated by measuring the absorbance of the formazan compounds produced in the cells. HDFn and HEKn cells were seeded at a concentration of  $1 \times 10^5$  cells/well in a 96-well plate, and after 3 and 24 h, they were treated with CRM-PMs. CRM-PMs concentrations of 2, 10, 50, and 100 µg/mL were administered for 6, 12, 24, and 48 h. Following CRM-PMs treatment, cells were cultured in a 5% CO<sub>2</sub>, 37 °C environment. Subsequently, media containing CRM-PMs were removed, and cells were washed twice with PBS. A solution of MTT (3-(4,5-Dimethylthiazol-2-yl)-2,5-diphenyltetrazolium) bromide, Thermo Fisher, Waltham, MA, USA) at a concentration of 5 mg/mL in PBS was added to each well at 10% (v/v) and incubated for 4 h. After incubation, a lysis buffer solution composed of 50% (w/v) N,N-dimethylformamide (DMF) and 10% (w/v) SDS was added to each well, and the generated formazan was allowed to dissolve at room temperature for 2 h. Absorbance at 570 nm was then measured using a microplate reader (Thermo Fisher Scientific, Waltham, MA, USA). The absorbance values of the MTT solution-containing media were subtracted from the absorbance values of each sample to process the results.

### 2.4. Measurement of Inflammatory Cytokine IL-8

To assess the inflammatory response of skin cells to fine dust, the expression levels of the inflammatory cytokine Interleukin 8 (IL-8) were determined. HDFn and HEKn cells were seeded at a concentration of  $5 \times 10^5$  cells/mL in a 48-well plate, and fine dust was cultured at a concentration of 50 µg/mL for 48 h. Culture supernatants were collected at 12 and 48 h and stored at −40 °C until further analysis. An in vitro enzyme immunoassay was performed using the Human IL-8 ELISA Kit (Abcam, Waltham, MA, USA). The media were mixed with antibody solutions and incubated on antibody plates at 37 °C for 2 h. After washing with PBS, a substrate solution (TMBZ solution) was added, and the reaction proceeded at room temperature for 20 min. The reaction was stopped by adding stop solution, and absorbance was measured at 450 nm using a microplate reader (Thermo Scientific, Waltham, MA, USA). The experimental procedures followed the protocol provided by the kit manufacturer, and the quantity of IL-8 was determined using the standard curve obtained from the IL-8 standard solution.

### 2.5. Analysis of Cell Behavior in Response to Fine Dust

To assess the pivotal actions of cells, particularly proliferation and migration, crucial for wound recovery, HEKn cells were employed. Initially, HEKn cells were seeded at a concentration of  $5 \times 10^5$  cells/well in a 48-well plate, and after 24 h, they were treated with fine dust at final concentrations of 2 and 50 µg/mL. Each experimental group was fixed at n = 5. Over a 7-day period, live cell imaging was conducted using a microscope (Nikon Eclipse Ti) at consistent coordinates, capturing cell images at 15-min intervals, alongside the control group without fine dust treatment. For cell proliferation, HEKn cell numbers were measured at 6, 12, 24, 48, and 72-h intervals. ImageJ (bundled with Java 8) was employed for image preprocessing to ensure uniformity and particle analysis for quantification, maintaining consistent measurement conditions. Subsequently, the measured cell numbers were divided by the area to analyze the cell density per unit area. Cell motility was evaluated using the Trackmate plugin in ImageJ, tracking cell

movement positions at 6, 12, 24, 36, and 48-h intervals. The analysis included assessing the distance covered during each time interval. Plugin settings and image preprocessing for cell movement distance analysis were standardized. Utilizing the recorded cell movement distances, the overall migration speed over time and instantaneous migration speed at 12-h intervals were analyzed, shedding light on the impact of fine dust composition and concentration on cell motility.

## 2.6. Analysis of Cytotoxicity and Growth Inhibition of Mixed Fine Dust

The composition of fine dust in the actual atmosphere varies depending on the season, location, and other factors. The effect of fine dust contained in the actual atmosphere, which consists of mixed components, on skin cells will be more complex than that of fine dusts of a single component. In this study, to determine differences in toxicity between individual fine dust model compounds and fine dust mixtures on skin cells, the effects of fine dust mixtures on the activity of skin cells were evaluated. The simulated composition of the fine dust mixture was based on representative atmospheric conditions during the winter in Seoul, Korea. The composition of representative fine dusts in Seoul (Seoul-PMs) is 22.6% of PM<sub>10</sub>-PAHs, 45.6% of PM<sub>10</sub>-Trace, and 31.7% of PM<sub>2.5</sub>-Ions [14]. To determine the effect of the Seoul-PMs, an MTT assay was performed on HEK293 cells at concentrations of 2 µg/mL and 50 µg/mL. In addition, in order to investigate the inhibitory effect of the model fine dusts used on the growth of HEK293 cells, the non-competitive inhibition model, which is one of the models that explains the inhibitory effect of bacterial growth, was used for analysis. Using this model equation, the growth inhibition constant ( $K_I$ ) and the reduced inhibition constant ( $\alpha$ ) were obtained for individual fine dusts [15].

$$\mu = \frac{\mu_m [S]}{K_m \left(1 + \frac{[I]}{K_I}\right) + [S] \left(1 + \frac{[I]}{K_I}\right)} \quad (1)$$

where,  $\mu$  and  $\mu_m$  are the specific growth rate and the maximum specific growth rate, respectively, and  $K_m$  and  $S$  are the saturation constant and substrate concentration, respectively. Moreover,  $[I]$  and  $K_I$  are the concentrations and the inhibition constant of an inhibitor (fine dusts), respectively. The reciprocal plot for the non-competitive inhibition model is as follows:

$$\frac{1}{\mu} \approx \frac{K_m}{\mu_m} \left(1 + \frac{[I]}{K_I}\right) \frac{1}{[S]} = \frac{K_m}{\mu_m [S]} \left(1 + \frac{[I]}{K_I}\right) \quad (2)$$

The inhibition constant for each of the fine dusts was obtained from the intercept ( $-K_I$ ) of the x-axis in a plot of  $1/\mu$  versus  $[I]$ . The concentration of individual or mixed inhibitors with different toxicities can be generalized to the concentration of the reference substance using the reduced inhibition constant ( $\alpha_i$ ) [15]

$$\alpha_i = \frac{K_{I,i}}{K_{I,Ref}} = \frac{[I]_i}{[I]_{Ref}} \quad (3)$$

where,  $K_{I,i}$  and  $K_{I,Ref}$  are the inhibition constants of the  $i$ -component and reference inhibitor, respectively, and  $[I]_i$  and  $[I]_{Ref}$  are the concentrations of the  $i$ -component and reference inhibitor, respectively.

## 2.7. Statistical Analysis

Students'  $t$ -tests were conducted using the R statistical programming environment. Bar graphs and scatter graphs with error bars indicate the mean and standard deviation.

## 3. Results and Discussion

### 3.1. Cytotoxicity of Skin Cells in Response to Fine Dust

The cytotoxic effects of fine dust on skin cells (HDFn and HEK293) were assessed using the MTT assay. Post-seeding stabilization periods of 3 h for HDFn and 12 h for HEK293

were followed by exposure to varied fine dust concentrations (2, 10, 50, 100  $\mu\text{g}/\text{mL}$ ) over 6, 12, 24, and 48 h. Cell viability, normalized to respective control groups, was measured through absorbance. The pre- and post-MTT treatment cell images for HDFn are detailed in Figure 1a. The control group showed a steady viability increase over 48 h (Figure 1b). In comparison, fine dust-exposed HDFn demonstrated a dose-dependent decrease in cell viability, which was particularly evident at 50  $\mu\text{g}/\text{mL}$  and higher concentrations (Figure 1c–e). At a low concentration of 2  $\mu\text{g}/\text{mL}$ , the cell viability of HDFn exposed to CRM-PM<sub>2.5</sub>-ions for 12 h decreased by 12.7% compared to the control group. Furthermore, the reduction in cell viability was 2.5 times greater than that observed with PAHs, a known carcinogenic component of fine dust. This underscores HDFn’s concentration-dependent cytotoxicity to fine dust, with smaller particle sizes exerting a greater impact. The direct influence of PM<sub>2.5</sub>-Ion composition on cellular toxicity is plausible, given its constituents, such as Na<sup>+</sup> and Ca<sup>2+</sup>. For HEKn viability measurements, pre- and post-MTT treatment cell images are illustrated in Figure 2a. The control group for untreated HEKn exhibited an 11.01% viability increase after 48 h, indicating gradual metabolic activity augmentation (Figure 2b). Similar to HDFn, HEKn exposed to fine dust showed reduced cell viability compared to their respective control groups at each time point (Figure 2c–e). HEKn displayed higher cytotoxicity than HDFn, especially when exposed to 2  $\mu\text{g}/\text{mL}$  of fine dust for 12 h, resulting in reductions of 25.76%, 34.02%, and 38.33% for PM<sub>10</sub>-PAHs, PM<sub>10</sub>-Trace, and PM<sub>2.5</sub>-Ions, respectively.

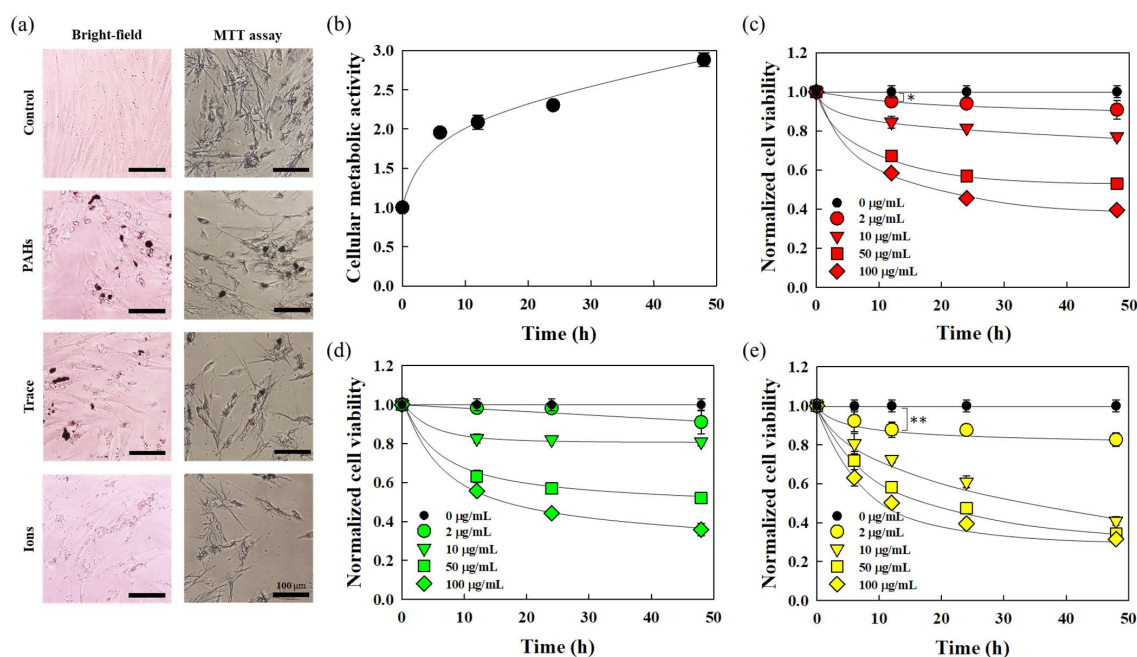


**Figure 1.** Cytotoxicity characterization of human dermal Fibroblasts (HDFn) by particulate matters. (a) Bright-field images of HDFn cells treated with 50  $\mu\text{g}/\text{mL}$  of PMs before and after the MTT assay. (b) Cellular metabolic activity measured at each time, normalized to the metabolic activity characterized right after cell stabilization in the well. (c) Cell viability measured at each time, normalized to the characterized pure medium group at each time, comparing different concentrations of (c) PAHs, (d) Trace, and (e) Ions (\*  $p < 0.05$ , \*\*  $p < 0.005$ ).

Examining the initial cytotoxic impact on both skin cell types and evaluating HDFn and HEKn cytotoxicity over 48 h of prolonged exposure reveals that HDFn’s cell viability decreases with increasing concentrations of PM<sub>10</sub>-PAHs and PM<sub>10</sub>-Trace. This is consistent with cell viability being dependent on fine dust concentration [16] and cytotoxicity being induced by PM, depending on the dose and exposure time [17]. PM<sub>2.5</sub>-Ions, however, maintain relatively stable cell viability beyond 10  $\mu\text{g}/\text{mL}$ . Moreover, at higher concentrations, cell viability converges to around 0.4. Conversely, HEKn, irrespective of the fine dust type,

exhibits approximately 0.5 cell viability up to 10 µg/mL. However, at higher concentrations, PM<sub>10</sub>-PAHs and PM<sub>10</sub>-Trace tend to sustain cell viability, while PM<sub>2.5</sub>-Ions result in lower cell viability (Figure 3a,b). The two cells showed different cytotoxicity trends depending on the type of fine dust, which emphasizes the vulnerability of HEK<sub>n</sub>, which forms the outermost layer of the skin, especially since cytotoxicity is associated with the overproduction of nitric oxide (NO) [18], and NO is known to stimulate cell death [19]. NO inhibits the activity of PARP-1, a DNA repair protein [20], suggesting that HEK<sub>n</sub>, which are susceptible to fine dust, may experience prolonged skin damage and slower recovery from exposure to fine dust during wound healing or skin conditions. The barrier of the skin epidermis is formed by tight junctions, making it difficult for external substances to penetrate healthy skin. However, these results indicate that when fine dust penetrates unhealthy or wounded skin, the epidermis sustains greater damage from the fine dust compared to the dermis. This suggests that recovery of the skin barrier may be challenging, potentially leading to a deterioration in skin health.

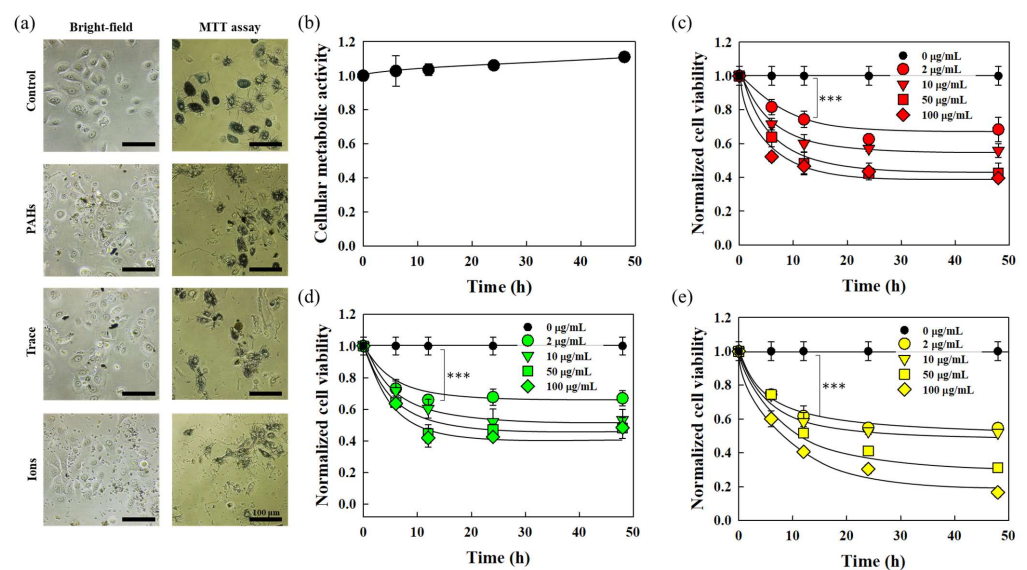


**Figure 2.** Cytotoxicity characterization of human epidermal keratinocytes (HEK<sub>n</sub>) by particulate matters. (a) Bright-field images of HEK<sub>n</sub> cells treated with 50 µg/mL of PMs before and after the MTT assay. (b) Cellular metabolic activity measured at each time, normalized to the metabolic activity characterized right after cell stabilization in the well. (c) Cell viability measured at each time, normalized to the characterized pure medium group at each time, comparing different concentrations of (c) PAHs, (d) Trace, and (e) Ions (\*\**p* < 0.0005).

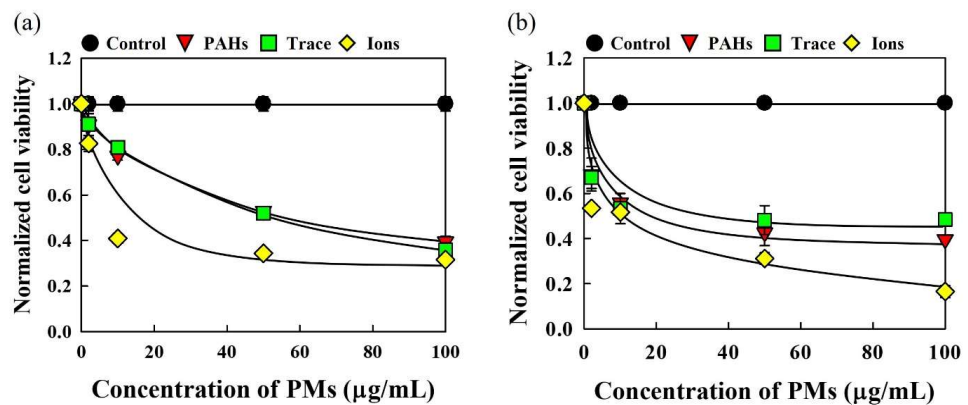


**Figure 3.** Assessing the impact of cells on particulate matters. Compare cell viability with each type of fine dust concentration after 48 h in (a) HDF<sub>n</sub> and (b) HEK<sub>n</sub>.

### 3.2. Evaluation of Inflammatory Cytokine Expression Induced by Fine Dust

Fine dust, by compromising the skin's epidermal barrier function and triggering immune responses, induces inflammatory reactions associated with allergen activation [21]. Among the various pro-inflammatory cytokines and chemokines generated during this process, IL-8, specifically secreted upon stimulation, plays a crucial role [22]. It recruits polymorphonuclear cells, such as immune cells and neutrophils, to the inflammatory site, directly influencing functions like cell death and proliferation in skin cells [23]. Therefore, to assess the inflammatory response of skin cells to fine dust, a quantitative analysis of IL-8 secretion was conducted. Both HDFn and HEKn exhibited an increase in IL-8 expression over time, even without exposure to fine dust, with HDFn displaying more vigorous basal IL-8 expression than HEKn. When comparing the IL-8 expression levels of both skin cells exposed to fine dust, it was observed that HEKn responded more sensitively to all types of fine dust than HDFn. Examining HDFn's IL-8 expression, it was noted that PM<sub>10</sub>-PAHs and PM<sub>10</sub>-Trace exhibited relatively minimal stimulation compared to PM<sub>2.5</sub>-Ions. Furthermore, when exposed to PM<sub>10</sub>-PAHs and PM<sub>10</sub>-Trace, the initial 12-h expression was higher than subsequent periods, while cells exposed to PM<sub>2.5</sub>-Ions displayed increased expression after 12 h (Figure 4a). In contrast, HEKn exhibited an increase in IL-8 expression after 12 h when exposed to PM<sub>10</sub>-PAHs and PM<sub>10</sub>-Trace, while cells exposed to PM<sub>2.5</sub>-Ions showed higher expression in the initial 12 h (Figure 4b). Notably, the decrease in IL-8 expression after 12 h of exposure to PM<sub>2.5</sub>-Ions may be attributed to reduced cell viability due to exposure to 50 µg/mL of PM<sub>2.5</sub>-Ions, leading to cell death [24]. Living cells, when exposed to stimuli or danger signals, induce necrosis or apoptosis, accompanied by inflammatory responses [25]. Along with cytokines, the resulting oxidative stress occurs when cells produce free radicals, which oxidize DNA and cause cells to become necrotic [26]. When oxidative stress is triggered, cells with reduced antioxidant capacity react with cell membranes, fatty acids, and proteins with excess free radicals, damaging cell function and DNA, leading to disease [27]. In summary, considering cell viability and the expression of the inflammatory cytokine IL-8, fine dust stimulation induces cell death, triggering an inflammatory response and activating the production of inflammatory cytokines. The higher cell survival rate in HDFn due to fine dust exposure may explain the comparatively lower IL-8 expression than in HEKn. Moreover, the higher absolute expression of IL-8 measured in the dermis suggests that if fine dust penetrates the dermis, it could induce a more substantial inflammatory response.

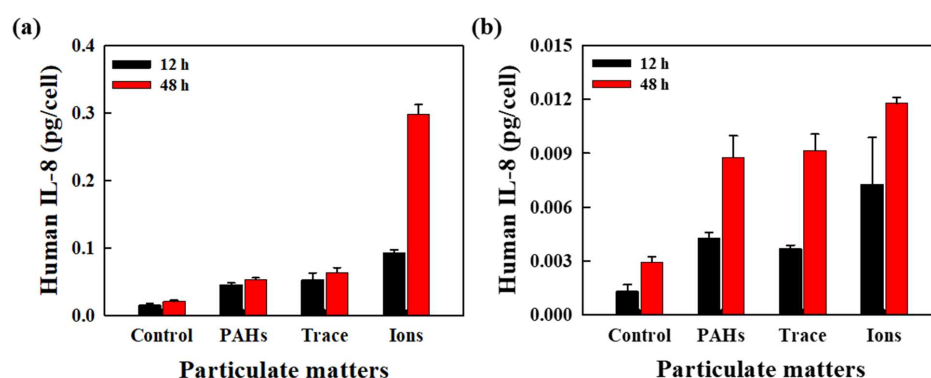


**Figure 4.** Assessing metabolic activity induced by particulate matters. Expression levels of the particulate matter-induced pro-inflammatory cytokine IL-8 in (a) HDFn and (b) HEKn cells. IL-8 expression was assessed after treatment with 50 µg/mL of particulate matter and expressed IL-8 levels were evaluated per cell.

### 3.3. Proliferative Characteristics of HEKn in Response to Fine Dust

While metabolic activity of skin cells in response to fine dust was confirmed through cell survival assessments via MTT assay and cytokine evaluations based on IL-8 secretion, the dynamic behaviors influenced by cell proliferation, such as monolayer formation and cell

migration, cannot be evaluated. As the epidermal layer-forming HEK<sub>n</sub> creates a monolayer with tight junctions, visually analyzing and quantifying the differences between fine dust-exposed cells and normal cells are crucial. Thus, in this study, HEK<sub>n</sub> was treated with fine dust, and changes over time following 72 h of exposure were monitored using live cell imaging equipment. To assess the proliferation rate and monolayer formation of HEK<sub>n</sub>, cell density per unit area was measured. The cell density of the control group, untreated with fine dust, increased 3.2 times from the initial measurement to  $956.63 \pm 33.49$  cells/mm<sup>2</sup> after 72 h. Fine dust-exposed HEK<sub>n</sub> showed a lower cell density compared to the control group, with PM<sub>2.5</sub>-Ions exhibiting the lowest density, 1.8 times lower than the control group (Figure 5a). PM<sub>10</sub>-PAHs and PM<sub>10</sub>-Trace displayed cell densities slightly lower than the control group but higher than PM<sub>2.5</sub>-Ions. HEK<sub>n</sub> treated with 50 µg/mL displayed significantly lower cell density than those exposed to 2 µg/mL (Figure 5b), indicating that higher fine dust concentrations reduce cell proliferation rates. In particular, HEK<sub>n</sub> exposed to PM<sub>2.5</sub>-Ions showed a 3.4 times lower proliferation rate compared to the control group, indicating that smaller particle sizes have a greater impact. Quantifying proliferation rates through cell counts revealed that higher fine dust concentrations lead to decreased proliferation, especially for PM<sub>2.5</sub>-Ions, which showed 1.6 times lower at 2 µg/mL and 2.8 times lower at 50 µg/mL compared to the control group.

Exposure to fine dust particles induces oxidative stress, inflammation, and DNA damage in cells [28], and these cellular responses can disrupt normal cellular metabolic activity and affect the rate of cell proliferation. The findings also support the concept that PAHs, trace elements, and ions in particulate matter directly affect cell viability and proliferation [29]. PAHs and trace-element fine dusts, as insoluble substances, appear to cause significant physical damage to cells, thereby reducing cell viability. Additionally, by occupying areas where cells need to proliferate, these fine dusts hinder adhesion with substrates essential for cell survival and proliferation, thus affecting the proliferation rate. Furthermore, fine dusts containing ionic components, which include some soluble substances, seem to cause both physical and chemical damage, thereby reducing both cell viability and proliferation rate. Exposure to fine dust has been associated with the expression of pro-inflammatory cytokines and chemokines [30], suggesting that fine dust further modulates cellular responses and potentially affects cell proliferation rates. In summary, the analysis of cell density and proliferation rates confirms that HEK<sub>n</sub> is influenced by fine dust exposure, aligning with the quantitative data analyzed through live cell imaging and the trend observed in MTT assay cell survival. Notably, lower concentrations dominate in components and particle size, while higher concentrations significantly impair proliferation regardless of components. These results suggest potential effects on wound healing rates due to impacts on monolayer formation and tight junctions.

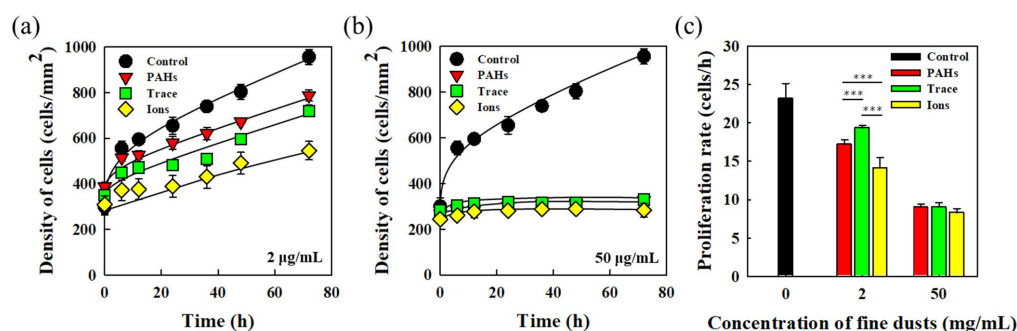


**Figure 5.** Characterization of HEK<sub>n</sub> proliferation rate induced by fine dusts. HEK<sub>n</sub> cells were imaged using live cell imaging and analyzed with ImageJ. Each fine dust material was treated at concentrations of (a) 2 µg/mL and (b) 50 µg/mL, then compared to the control. (c) Proliferation rates of HEK<sub>n</sub> cells at 48 h were assessed (\*\**p* < 0.0005).



### 3.4. Analysis of HEK<sub>n</sub> Migration in Response to Fine Dust

Observations through live cell imaging confirmed that cell migration is affected by fine dust, in addition to its impact on cell proliferation. Cell movement is a crucial process for cells to adapt to their environment and reach appropriate positions for functional purposes. Cell migration is regulated by a variety of molecular processes, including changes in cell shape, cell structural arrangement, adhesion, and interactions with the extracellular matrix [31], and growth factors, cytokines, and chemokines contribute to regulating cell migration [32]. This cellular movement and these mechanical changes play a key role in various biological processes, including tissue formation, immune defense, inflammation, and cancer progression [33]. Therefore, the influence of fine dust on the migration of skin cells was analyzed using live cell imaging, capturing HEK<sub>n</sub> responsible for the skin barrier function over 48 h at 15-min intervals. Quantitative analysis of parameters such as displacement distance and velocity was conducted using the Trakmate plugin in ImageJ (Figure 6a). Fine dust-exposed HEK<sub>n</sub> exhibited shorter displacement distances compared to the control group. Notably, cells exposed to 50 µg/mL of fine dust showed significantly shorter displacement distances than those exposed to 2 µg/mL, indicating a concentration-dependent effect (Figure 6b). Particularly, samples exposed to PM<sub>2.5</sub>-Ions, characterized by smaller particle sizes, consistently displayed the shortest displacement distances at all concentrations. Cells exposed to 50 µg/mL of PM<sub>2.5</sub>-Ions exhibited an 11.4-fold reduction in displacement distance compared to the control group. These results suggest that cellular damage and oxidative stress act within the cell and affect cell migration [34]. Fine dust, especially with smaller particle sizes, not only lowers cell survival but also influences cell movement and activity. The impact of fine dust concentration and particle size on cell mobility was evident in HEK<sub>n</sub>, indicating that higher concentrations and smaller particle sizes result in reduced cell movement. Moreover, restricting cell migration is the same as weakening cell migration due to exposed particles altering cell morphology and limiting cell range of motion [35]. Additionally, momentary movement speeds were analyzed at 6 and 12-h intervals to assess the temporal dynamics of cell migration. Unexposed cells showed an initial increase in movement speed up to 24 h, followed by a decrease. This phenomenon could be attributed to increased cell numbers during HEK<sub>n</sub> proliferation, causing cells to be surrounded and movement to decrease. This is equivalent to saying that when a cell is exposed to certain stimuli or stressors, it can undergo rapid proliferation in response to repair and regeneration signals by the cell's defense mechanisms [36]. However, if a cell is constantly stimulated by external and stressful factors, it may inhibit cell proliferation or cause cell death as a programmed protective response mechanism [37,38].

Examination of the movement speed of HEK<sub>n</sub> exposed to 2 µg/mL of fine dust revealed faster movement compared to the control group up to 12 h, followed by a gradual reduction in speed (Figure 6c). For cells exposed to 50 µg/mL, a significant reduction in movement speed was observed compared to 2 µg/mL (Figure 6d). Notably, PM<sub>2.5</sub>-Ions at 50 µg/mL showed movement speeds 2.1 times slower than the control group up to 24 h, suggesting that higher concentrations of fine dust hinder both cell survival and movement. This means that when a cell is exposed to certain toxins or DNA-damaging agents, to prevent the proliferation of damaged cells, the cell activates cellular checkpoint mechanisms [39], stopping cell division or inducing apoptosis [40], and inhibiting migration and proliferation. The recovery and regeneration of the epidermis proceed through a process where the proliferation of keratinocytes leads to the formation of the basal layer, followed by their differentiation to stratum corneum. The introduction of fine dust hinders keratinocyte proliferation, slowing down basal layer formation, and acts as a defect in the tight junctions within the basal layer, thereby weakening structural integrity. Additionally, cell death caused by fine dust creates debris, which can further contribute to these defects, leading to secondary damage. These processes slow down skin recovery and regeneration, and prolonged exposure may alter cellular metabolic activity and ultimately result in tissue deformation. Therefore, these findings demonstrate that various cellular behaviors—including not only cytotoxicity but also migration, proliferation, and other

behaviors—are all affected, which significantly impacts the recovery and regeneration of skin tissue.

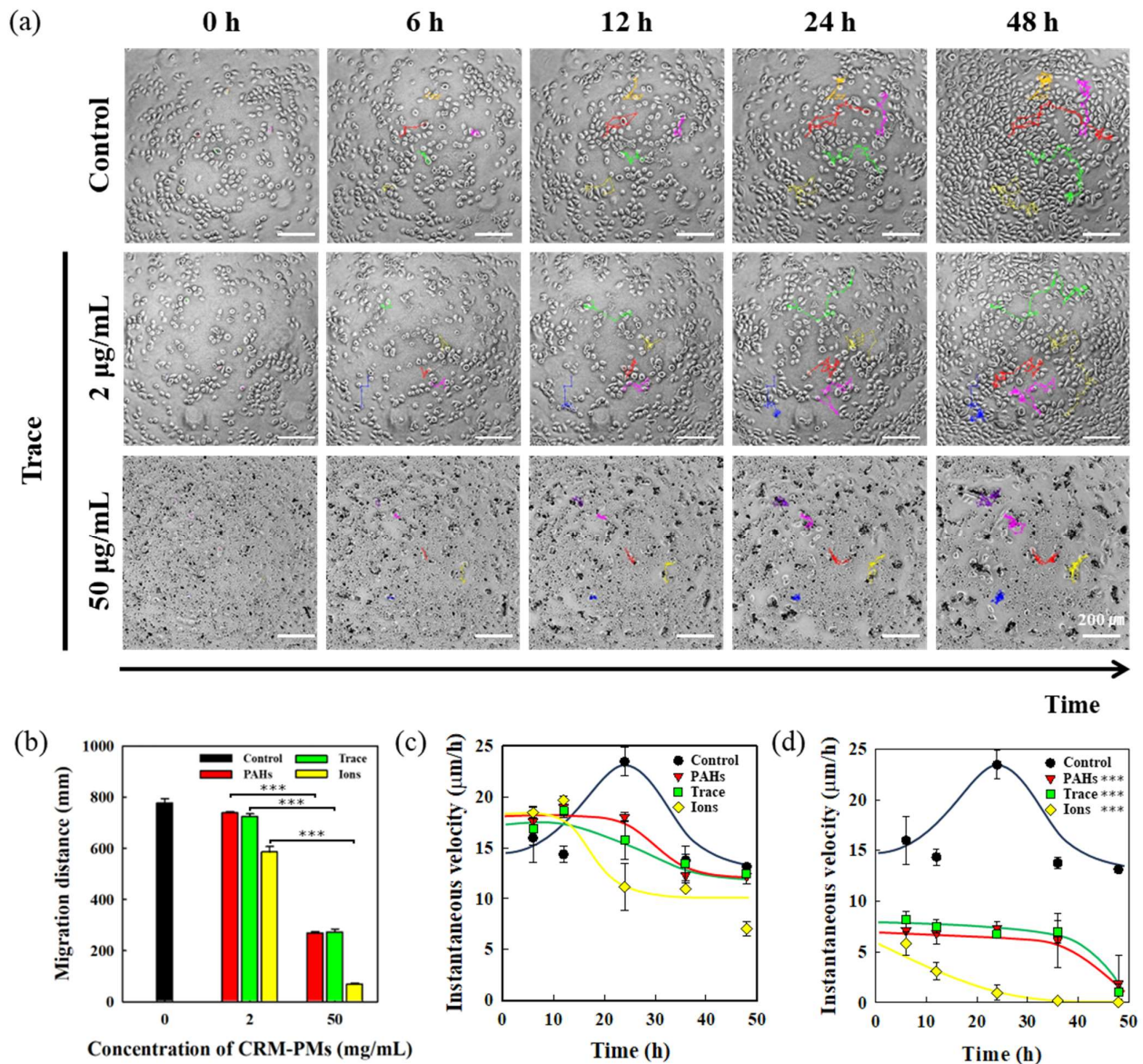


**Figure 6.** Analysis of the behavior of HEK293T affected by particulate matter. **(a)** HEK293T activity in each fine dust component was analyzed by ImageJ. **(b)** The migration distance of HEK293T treated with each particulate matter was analyzed compared to the control. HEK293T were treated with 2 µg/mL and 50 µg/mL concentrations of each particulate matter for 48 h and analyzed (\*\*\*)  $p < 0.0005$ ). The hourly proliferation instantaneous rate of HEK293T by particulate matter was evaluated by treating **(c)** 2 µg/mL and **(d)** 50 µg/mL of each material. The asterisks in **(d)** indicate statistical significance compared to the 2 µg/mL group (\*\*\*)  $p < 0.0005$ .

### 3.5. Correlation Analysis of HEK293T Metabolic and Behavioral Characteristics in Response to Fine Dust

A comprehensive analysis of the impact of fine dust on HEK293T cells was conducted by integrating results from cell viability, IL-8 secretion, proliferation, and migration assessments. The correlation between MTT assay-derived cell viability and proliferation, reflecting actual proliferation rates and cell density, was investigated (Figure 7a). Despite slight variations depending on the type of fine dust, a linear trend indicated that both cell viability and proliferation increase as concentrations decrease. Additionally, the correlation

between HEK293T's migration speed, proliferation rate, and the IL-8 inflammatory response factor was examined (Figure 7b). The migration and proliferation rates of HEK293T exponentially declined as fine dust concentrations decreased. This suggests that fine dust not only hinders cell proliferation and movement but also impairs cell viability. Conversely, IL-8 secretion decreased as fine dust concentrations decreased. The danger signal from fine dust induces necrosis and apoptosis, triggering inflammatory responses in cells. Thus, the increased IL-8 secretion, reduced proliferation and migration, and cell death collectively indicate the influence of fine dust. This emphasizes that cell viability assessments can predict proliferation, movement, and metabolic activity of HEK293T cells.

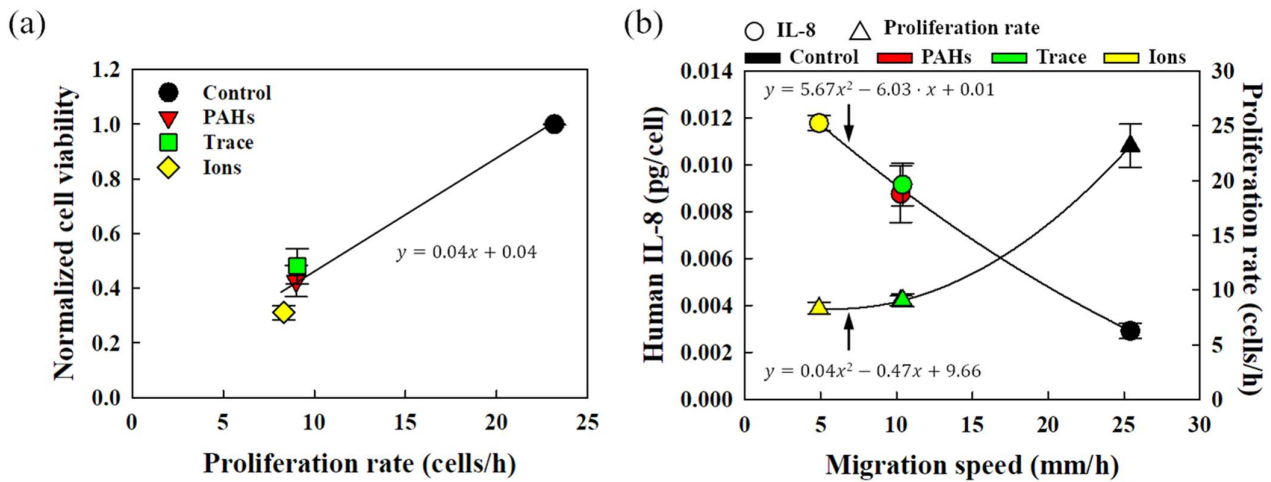


**Figure 7.** Correlation between metabolic activity toward fine dust and morphological analysis of HEK293T. (a) Proliferation rate and cell survival rate. (b) Correlation between cell migration speed and proliferation rate and IL-8 secretion. The correlation between metabolic activity and morphological analysis of HEK293T responding to particulate matter was evaluated. The injection amount of each PM was 50 µg/mL, and each analysis item was evaluated for 48 h.

### 3.6. Cytotoxicity and Growth Inhibition of Mixed Fine Dust

The specific growth rate and inhibitory effect of HEK293T cells according to changes in the concentration of fine dusts are shown in Figure 8a. In the control group where PMs were not added, the growth rate of HEK293T cells was about 0.03 d<sup>-1</sup>. The growth rate was inhibited as the PMs concentration increased. At 50 µg/mL, the growth rate was approximately 0.004~0.009 d<sup>-1</sup> depending on the species of PMs, which was reduced by approximately 68~87% compared to the control group. As a result of analyzing the inhibition mechanism using experimental data on the growth rate of HEK293T cells according to the concentration change of individual PMs, the inhibitory action of the three PM models was interpreted as a non-competitive inhibition model (Equation (1)).

In this paper, PM<sub>2.5</sub>-Ions, which have the strongest inhibitory effect on HEK293T cells, were selected as the reference inhibitor. Using experimental data on the cell growth of HEK293T cells exposed to various concentrations of fine dusts,  $K_{I,i}$  and  $\alpha_i$  for each fine dust obtained from Equations (2) and (3) are summarized in Table 1. In addition, the two concentrations (low and high) of the Seoul-PMs were converted to the concentration of PM<sub>2.5</sub>-Ions, a reference material, using the following Equation (4), and the reduced PM<sub>2.5</sub>-Ions concentration is presented in Table 1.

$$[I]_{Reduced\ PM-Ions} = \sum \frac{[I]_i}{\alpha_i} \quad (4)$$

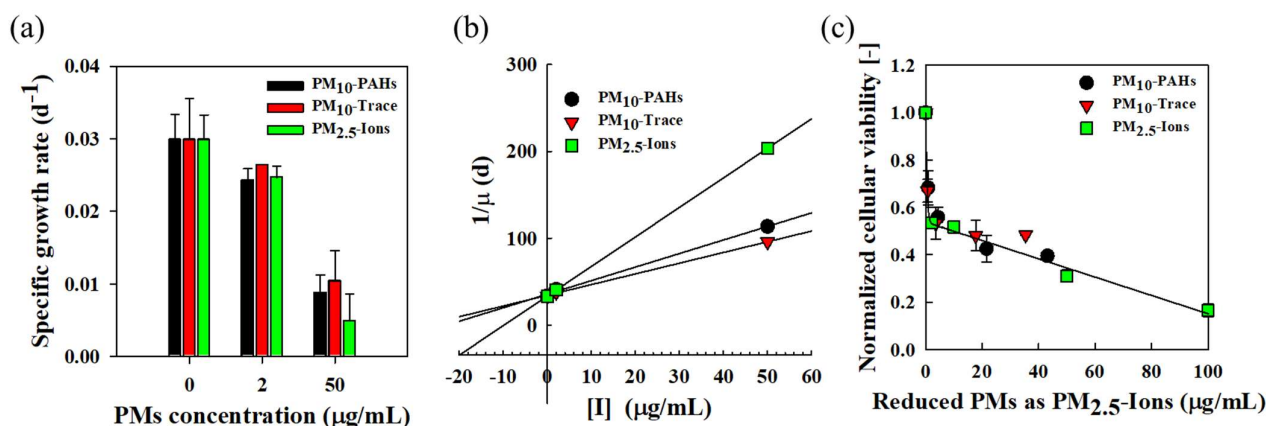


**Figure 8.** Specific growth rate of HEK293 cells according to changes in PM concentration (a), plot of [I] and 1/μ by non-competitive inhibition model (b) and normalized cell viability with the reduced PMs (c) (from Figure 3b).

**Table 1.** The inhibition constant ( $K_{I,i}$ ) and the reduced inhibition constant ( $\alpha_i$ ) of fine dusts on HEK293 cells and concentration of the simulated Seoul-PMs.

CRM-PMs	$K_{I,i}$ (μg/mL)	$\alpha_i$ [-]	Composition of Representative Seoul-PMs (%) [14]	Concentration of Simulated Seoul-PMs (μg/mL)		Reduced Concentration of the Seoul-PMs as PM <sub>2.5</sub> -Ions (μg/mL)	
				Low PMs	High PMs	Low PMs	High PMs
PM <sub>10</sub> -PAHs	22.9	2.32	22.6	0.45	11.30	0.20	4.87
PM <sub>10</sub> -Trace	27.9	2.82	45.6	0.91	22.80	0.32	8.06
PM <sub>2.5</sub> -Ions	9.9	1.00	31.7	0.64	15.85	0.63	15.85
Total			100.0	2.00	50.00	1.15	28.78

The inhibition constant for each fine dust and the reduced inhibition constant evaluated using the most toxic PM<sub>2.5</sub>-Ions as the reference material are summarized in Table 1. The smaller the inhibition constant, the stronger the toxicity of fine dusts. The toxicity of fine dusts to HEK293 cells is in the following order: PM<sub>2.5</sub>-Ions, PM<sub>10</sub>-PAHs, and PM<sub>10</sub>-Trace.

The normalized cellular viability of HEK293 cells (Figure 3b) according to changes in the concentrations of three types of PMs was redrawn based on the reduced PMs concentration converted to the concentration of PM<sub>2.5</sub>-Ions, a reference substance, using the reduced inhibition constant (Figure 8c). Despite the different toxicity of each PM, the cellular viability of each PMs was similar when the reduced PMs concentration was the same. These results suggest that the toxicity of each PMs can be generalized to that of the reference substance by using the reduced inhibition constant, even if the toxicity is different. As shown in Table 1, Figure 9 shows the cellular viability of HEK293 cells according to the concentration change of Seoul-PMs, which simulates the composition of PMs in the air of typical Seoul during the winter. The normalized cellular viability was about 0.66 at low concentration of Seoul-PM (2 μg/mL) and about 0.53 at high concentration of Seoul-PM (50 μg/mL). The cellular viability in Low Seoul-PMs (2 μg/mL) was similar to that of PM<sub>10</sub>-PAHs and PM<sub>10</sub>-Trace at the same concentration and was higher than that of PM<sub>2.5</sub>-Ions. The cellular viability of high Seoul-PMs (50 μg/mL) was higher than that of the three types of PMs at the same concentration. The concentrations of the reduced PM, which is a mixture of low concentration (2 μg/mL) and high concentration (50 μg/mL) of Seoul-PMs converted to PM<sub>2.5</sub>-Ions, are 1.15 and 28.78 μg/mL, respectively. When the concentration of PM<sub>2.5</sub>-Ions was 1.15 and 28.78 μg/mL, the predicted cellular viability was 0.66 and 0.53, respectively, but the viability of HEK293 cells exposed to the same concentration of Seoul-PMs was higher (Figure 9b).

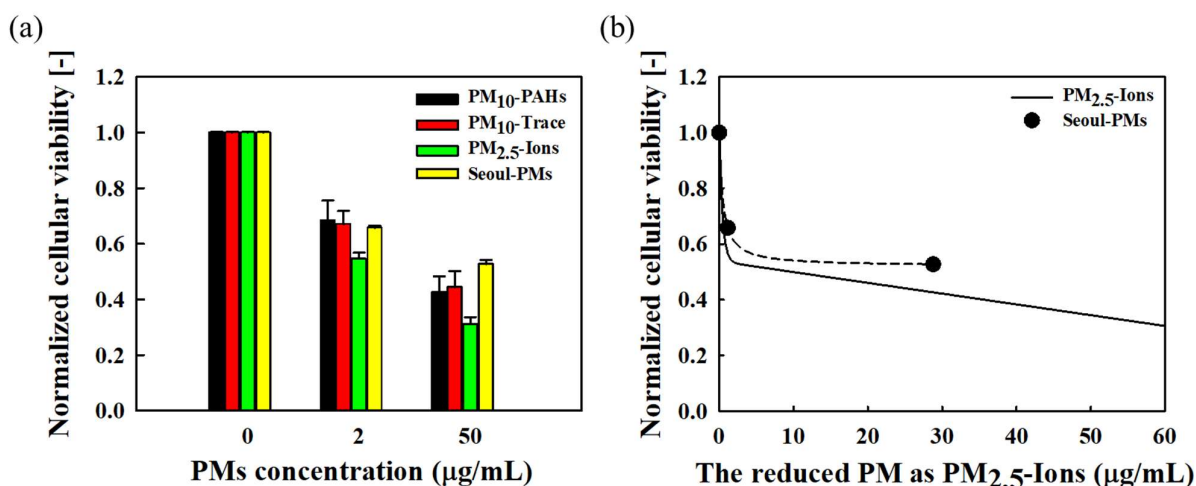


**Figure 9.** Normalized cellular viability of HEK293 cells according to changes in the concentration of Seoul-PMs. (a) PMs concentration and (b) the reduced PMs as PM<sub>2.5</sub>-Ions.

The results in Figures 8 and 9 demonstrate that: (1) The individual inhibitory actions of substances with different levels of cytotoxicity are determined by using an appropriate inhibition model equation to determine the inhibition constant and the reduced inhibition constant; (2) The concentration of individual toxic substances can be converted from the reduced inhibition constant to the reference inhibitor concentration; and (3) Ultimately, the toxicity of each toxic substance can be generalized to the toxicity (inhibitory action) of the reference substance, and a comparative analysis of each toxicity is possible. The reduced inhibition constant is derived from inhibition model equations to analyze the growth inhibition (enzyme activity inhibition) effect of toxic substances on microorganisms. This study is the first case of applying this inhibition model to human cells and air pollutants, suggesting that it is useful not only for microorganisms such as bacteria and yeast, but also for human and animal cells.

Although many studies have investigated the physiological effects of fine dust on cells, it is challenging to identify offset effects or synergistic effects between specific toxic substances due to the mixture of various components [41,42]. However, this will be very useful in understanding the toxicity of mixtures as well as single toxic substances. The relative toxicity of single substances can be evaluated by comparing the values of each inhibition constant. If the concentration of each toxic substance is converted to the concentration of the reference substance using the reduced inhibition constant, the toxicity of a substance can be directly compared with that of various toxic substances. The toxicity of a mixture acts as a weight corresponding to the concentration and inherent toxicity of each substance constituting the mixture or causes a synergy effect or offset effect between the toxic substances constituting the mixture. From Figure 9b, which is the result obtained by applying this method, it can be seen that the mixture Seoul-PM shows an offsetting effect of displaying lower toxicity than the inherent toxicity of each constituent PM toward HEK293 cells.

#### 4. Conclusions

In this study, the physiological effects of fine dust on skin cells were analyzed based on their behavioral characteristics. Even at minimal concentrations, fine dust substantially hindered the growth of both HEK293 and HDFn cells, with PM<sub>2.5</sub>-Ions exerting the most pronounced effects. Notably, HEK293 displayed heightened sensitivity to fine dust, consistently eliciting inflammatory responses across all fine dust components, as is particularly evidenced by elevated IL-8 expression in PM<sub>2.5</sub>-Ions. Moreover, behavioral analyses of HEK293 unveiled diminished cell density, proliferation rates, and migration distances, notably accentuated at a high PM<sub>2.5</sub>-Ions concentration (50 µg/mL). Interestingly, a simulated mixed

model mirroring Seoul's atmospheric fine dust composition revealed reduced cellular toxicity compared to individual components, underscoring the complexity of real-world fine dust interactions. The findings collectively underscore that fine dust elicits inflammation in skin cells, precipitating reduced proliferation, migration, and heightened cell mortality. This comprehensive understanding illuminates the intricate interplay between fine dust exposure and skin cell responses, offering promising avenues for further exploration into cellular metabolism and behavior under environmental stressors. Overall, this study, which contributes to addressing the skin health risks posed by air pollutants, could be actively used in environmental science, dermatology, and public health.

**Supplementary Materials:** The following supporting information can be downloaded at: <https://www.mdpi.com/article/10.3390/environments1110259/s1>, Table S1: Composition of CRM-PM10-PAHs. Table S2: Composition of CRM-PM10-Trace. Table S3. Composition of CRM-PM10-Ions.

**Author Contributions:** T.E.K. and J.W.L. have contributed equally to this study. J.H.J. and H.W.R. conceptualization; T.E.K. and J.W.L. investigation and data acquisition; T.E.K. and J.W.L. formal analysis; T.E.K., J.W.L., J.H.J. and H.W.R. writing manuscript; J.H.J. and H.W.R. funding acquisition. All authors have read and agreed to the published version of the manuscript.

**Funding:** This study was supported by the National Research Foundation of Korea (RS-2024-00358960) and by the Ministry of Education (NRF-2020R1A6A1A03044977).

**Data Availability Statement:** The original contributions presented in this study are included in the article/Supplementary Materials. Further inquiries can be directed to the corresponding authors.

**Conflicts of Interest:** The authors declare no conflicts of interest.

## References

1. Shaddick, G.; Thomas, M.L.; Mudu, P.; Ruggeri, G.; Gumy, S. Half the world's population are exposed to increasing air pollution. *npj Clim. Atmos. Sci.* **2020**, *3*, f23. [[CrossRef](#)]
2. Fitoussi, R.; Faure, M.-O.; Beauchef, G.; Achard, S. Human skin responses to environmental pollutants: A review of current scientific models. *Environ. Pollut.* **2022**, *306*, 119316. [[CrossRef](#)] [[PubMed](#)]
3. Hamra Ghassan, B.; Guha, N.; Cohen, A.; Laden, F.; Raaschou-Nielsen, O.; Samet Jonathan, M.; Vineis, P.; Forastiere, F.; Saldiva, P.; Yorifuji, T.; et al. Outdoor Particulate Matter Exposure and Lung Cancer: A Systematic Review and Meta-Analysis. *Environ. Health Perspect.* **2014**, *122*, 906–911. [[CrossRef](#)] [[PubMed](#)]
4. Pope, C.A.; Burnett Richard, T.; Turner Michelle, C.; Cohen, A.; Krewski, D.; Jerrett, M.; Gapstur Susan, M.; Thun Michael, J. Lung Cancer and Cardiovascular Disease Mortality Associated with Ambient Air Pollution and Cigarette Smoke: Shape of the Exposure–Response Relationships. *Environ. Health Perspect.* **2011**, *119*, 1616–1621. [[CrossRef](#)] [[PubMed](#)]
5. Saw, C.L.L.; Yang, A.Y.; Huang, M.T.; Liu, Y.; Lee, J.H.; Khor, T.O.; Su, Z.Y.; Shu, L.; Lu, Y.; Conney, A.H.; et al. Nrf2 null enhances UVB-induced skin inflammation and extracellular matrix damages. *Cell Biosci.* **2014**, *4*, 39. [[CrossRef](#)]
6. Parrado, C.; Mercado-Saenz, S.; Perez-Davo, A.; Gilaberte, Y.; Gonzalez, S.; Juarranz, A. Environmental Stressors on Skin Aging. Mechanistic Insights [Review]. *Front. Pharmacol.* **2019**, *10*, 759. [[CrossRef](#)]
7. Kelly, F.J.; Fussell, J.C. Size, source and chemical composition as determinants of toxicity attributable to ambient particulate matter. *Atmos. Environ.* **2012**, *60*, 504–526. [[CrossRef](#)]
8. Valavanidis, A.; Fiotakis, K.; Vlachogianni, T. Airborne Particulate Matter and Human Health: Toxicological Assessment and Importance of Size and Composition of Particles for Oxidative Damage and Carcinogenic Mechanisms. *J. Environ. Sci. Health Part C* **2008**, *26*, 339–362. [[CrossRef](#)]
9. Jindal, S.; Chaudhary, Y.; Aggarwal, K.K. Toxicity of polyaromatic hydrocarbons and their biodegradation in the environment. In *Green Chemistry Approaches to Environmental Sustainability*; Elsevier: Amsterdam, The Netherlands, 2024; pp. 43–66.
10. Sombiri, S.; Balhara, N.; Attri, D.; Kharb, I.; Giri, A. An overview on occurrence of polycyclic aromatic hydrocarbons in food chain with special emphasis on human health ailments. *Discov. Environ.* **2024**, *2*, 87. [[CrossRef](#)]
11. Coxon, T.; Goldstein, L.; Odhiambo, B.K. Analysis of spatial distribution of trace metals, PCB, and PAH and their potential impact on human health in Virginian Counties and independent cities, USA. *Environ. Geochem. Health* **2019**, *41*, 783–801. [[CrossRef](#)]
12. Glencross, D.A.; Ho, T.-R.; Camiña, N.; Hawrylowicz, C.M.; Pfeffer, P.E. Air pollution and its effects on the immune system. *Free Radic. Biol. Med.* **2020**, *151*, 56–68. [[CrossRef](#)]
13. Wang, L.; Lee, W.; Cui, Y.R.; Ahn, G.; Jeon, Y.-J. Protective effect of green tea catechin against urban fine dust particle-induced skin aging by regulation of NF- $\kappa$ B, AP-1, and MAPKs signaling pathways. *Environ. Pollut.* **2019**, *252*, 1318–1324. [[CrossRef](#)]
14. gon Ryou, H.; Heo, J.; Kim, S.Y. Source apportionment of PM10 and PM2.5 air pollution, and possible impacts of study characteristics in South Korea. *Environ. Pollut.* **2018**, *240*, 963–972. [[CrossRef](#)]

15. Cho, K.-S.; Ryu, H.-W.; Choi, H.-M. Toxicity evaluation of complex metal mixtures using reduced metal concentrations: Application to iron oxidation by *Acidithiobacillus ferrooxidans*. *J. Microbiol. Biotechnol.* **2008**, *18*, 1298–1307. [[PubMed](#)]
16. Akhtar, U.S.; McWhinney, R.D.; Rastogi, N.; Abbatt JP, D.; Evans, G.J.; Scott, J.A. Cytotoxic and proinflammatory effects of ambient and source-related particulate matter (PM) in relation to the production of reactive oxygen species (ROS) and cytokine adsorption by particles. *Inhal. Toxicol.* **2010**, *22* (Suppl. 2), 37–47. [[CrossRef](#)] [[PubMed](#)]
17. Yang, X.; Feng, L.; Zhang, Y.; Hu, H.; Shi, Y.; Liang, S.; Zhao, T.; Fu, Y.; Duan, J.; Sun, Z. Cytotoxicity induced by fine particulate matter (PM<sub>2.5</sub>) via mitochondria-mediated apoptosis pathway in human cardiomyocytes. *Ecotoxicol. Environ. Saf.* **2018**, *161*, 198–207. [[CrossRef](#)] [[PubMed](#)]
18. Marmolino, D.; Manto, M. Pregabalin antagonizes copper-induced toxicity in the brain: In vitro and in vivo studies. *Neurosignals* **2011**, *18*, 210–222. [[CrossRef](#)] [[PubMed](#)]
19. Huang, Y.-C.T.; Soukup, J.; Harder, S.; Becker, S. Mitochondrial oxidant production by a pollutant dust and NO-mediated apoptosis in human alveolar macrophage. *Am. J. Physiol. Cell Physiol.* **2003**, *284*, C24–C32. [[CrossRef](#)]
20. Zhou, X.; Cooper, K.L.; Huestis, J.; Xu, H.; Burchiel, S.W.; Hudson, L.G.; Liu, K.J. S-nitrosation on zinc finger motif of PARP-1 as a mechanism of DNA repair inhibition by arsenite. *Oncotarget* **2016**, *7*, 80482. [[CrossRef](#)]
21. Kim, H.B.; Choi, M.G.; Chung, B.Y.; Um, J.Y.; Kim Jin, C.; Park, C.W.; Kim, H.O. Particulate matter 2.5 induces the skin barrier dysfunction and cutaneous inflammation via AhR- and T helper 17 cell-related genes in human skin tissue as identified via transcriptome analysis. *Exp. Dermatol.* **2023**, *32*, 547–554. [[CrossRef](#)]
22. Coquette, A.; Berna, N.; Vandenbosch, A.; Rosdy, M.; De Wever, B.; Poumay, Y. Analysis of interleukin-1 $\alpha$  (IL-1 $\alpha$ ) and interleukin-8 (IL-8) expression and release in in vitro reconstructed human epidermis for the prediction of in vivo skin irritation and/or sensitization. *Toxicol. Vitro.* **2003**, *17*, 311–321. [[CrossRef](#)] [[PubMed](#)]
23. Yoshizumi, M.; Nakamura, T.; Kato, M.; Ishioka, T.; Kozawa, K.; Wakamatsu, K.; Kimura, H. Release of cytokines/chemokines and cell death in UVB-irradiated human keratinocytes, HaCaT. *Cell Biol. Int.* **2008**, *32*, 1405–1411. [[CrossRef](#)] [[PubMed](#)]
24. Hetland, R.B.; Cassee, F.R.; Refsnes, M.; Schwarze, P.E.; Låg, M.; Boere AJ, F.; Dybing, E. Release of inflammatory cytokines, cell toxicity and apoptosis in epithelial lung cells after exposure to ambient air particles of different size fractions. *Toxicol. Vitro.* **2004**, *18*, 203–212. [[CrossRef](#)] [[PubMed](#)]
25. Huang, Y.; Xu, W.; Zhou, R. NLRP3 inflammasome activation and cell death. *Cell. Mol. Immunol.* **2021**, *18*, 2114–2127. [[CrossRef](#)]
26. Federico, A.; Morgillo, F.; Tuccillo, C.; Ciardiello, F.; Loguercio, C. Chronic inflammation and oxidative stress in human carcinogenesis. *Int. J. Cancer* **2007**, *121*, 2381–2386. [[CrossRef](#)]
27. Khansari, N.; Shakiba, Y.; Mahmoudi, M. Chronic inflammation and oxidative stress as a major cause of age-related diseases and cancer. *Recent Pat. Inflamm. Allergy Drug Discov.* **2009**, *3*, 73–80. [[CrossRef](#)]
28. Yuhong, H.; Thomas, C.; Sandrah, P.E.; Tingyu, Y.; Xinci, C.; Mario, V.; Nathan, P.; Fred, L.; Deborah, L.; Nathana, L.; et al. Joint effects of traffic-related air pollution and hypertensive disorders of pregnancy on maternal postpartum depressive and anxiety symptoms. *J. Expo. Sci. Environ. Epidemiol.* **2024**. [[CrossRef](#)]
29. Kermani, M.; Rahmatinia, T.; Oskoei, V.; Norzaee, S.; Shahsavani, A.; Farzadkia, M.; Kazemi, M.H. Potential cytotoxicity of trace elements and polycyclic aromatic hydrocarbons bounded to particulate matter: A review on in vitro studies on human lung epithelial cells. *Environ. Sci. Pollut. Res.* **2021**, *28*, 55888–55904. [[CrossRef](#)]
30. Leikauf, G.D.; Kim, S.-H.; Jang, A.-S. Mechanisms of ultrafine particle-induced respiratory health effects. *Exp. Mol. Med.* **2020**, *52*, 329–337. [[CrossRef](#)]
31. Luo, J.; Walker, M.; Xiao, Y.; Donnelly, H.; Dalby, M.J.; Salmeron-Sanchez, M. The influence of nanotopography on cell behaviour through interactions with the extracellular matrix—A review. *Bioact. Mater.* **2022**, *15*, 145–159. [[CrossRef](#)]
32. Weaver, D.F. Amyloid beta is an early responder cytokine and immunopeptide of the innate immune system. *Alzheimer's Dement. Transl. Res. Clin. Interv.* **2020**, *6*, e12100. [[CrossRef](#)] [[PubMed](#)]
33. Di, X.; Gao, X.; Peng, L.; Ai, J.; Jin, X.; Qi, S.; Li, H.; Wang, K.; Luo, D. Cellular mechanotransduction in health and diseases: From molecular mechanism to therapeutic targets. *Signal Transduct. Target. Ther.* **2023**, *8*, 282. [[CrossRef](#)] [[PubMed](#)]
34. Qing, Y.; Xiang, X.; Li, S.; Wang, M.; Liang, Z.; Ren, J. Integrated evaluation the antioxidant activity of epicatechin from cell dynamics. *Biotechnol. Prog.* **2023**, *39*, e3328. [[CrossRef](#)] [[PubMed](#)]
35. Cheng, Y.; Ren, J.; Fan, S.; Wu, P.; Cong, W.; Lin, Y.; Lan, S.; Song, S.; Shao, B.; Dai, W. Nanoparticulates reduce tumor cell migration through affinity interactions with extracellular migrasomes and retraction fibers. *Nanoscale Horiz.* **2022**, *7*, 779–789. [[CrossRef](#)]
36. Prudovsky, I. Cellular mechanisms of FGF-stimulated tissue repair. *Cells* **2021**, *10*, 1830. [[CrossRef](#)]
37. Bedoui, S.; Herold, M.J.; Strasser, A. Emerging connectivity of programmed cell death pathways and its physiological implications. *Nat. Rev. Mol. Cell Biol.* **2020**, *21*, 678–695. [[CrossRef](#)]
38. Cohen, S.M.; Ellwein, L.B. Cell Proliferation in Carcinogenesis. *Science* **1990**, *249*, 1007–1011. [[CrossRef](#)]
39. Campos, A.; Clemente-Blanco, A. Cell cycle and DNA repair regulation in the damage response: Protein phosphatases take over the reins. *Int. J. Mol. Sci.* **2020**, *21*, 446. [[CrossRef](#)]
40. Heydarnezhad Asl, M.; Pasban Khelejani, F.; Bahojb Mahdavi, S.Z.; Emrahi, L.; Jebelli, A.; Mokhtarzadeh, A. The various regulatory functions of long noncoding RNAs in apoptosis, cell cycle, and cellular senescence. *J. Cell. Biochem.* **2022**, *123*, 995–1024. [[CrossRef](#)]

41. Wei, H.; Yuan, W.; Yu, H.; Geng, H. Cytotoxicity induced by fine particulate matter (PM<sub>2.5</sub>) via mitochondria-mediated apoptosis pathway in rat alveolar macrophages. *Environ. Sci. Pollut. Res.* **2021**, *28*, 25819–25829. [[CrossRef](#)]
42. Wu, J.; Shi, Y.; Asweto, C.O.; Feng, L.; Yang, X.; Zhang, Y.; Sun, Z. Fine particle matters induce DNA damage and G2/M cell cycle arrest in human bronchial epithelial BEAS-2B cells. *Environ. Sci. Pollut. Res.* **2017**, *24*, 25071–25081. [[CrossRef](#)]

**Disclaimer/Publisher’s Note:** The statements, opinions and data contained in all publications are solely those of the individual author(s) and contributor(s) and not of MDPI and/or the editor(s). MDPI and/or the editor(s) disclaim responsibility for any injury to people or property resulting from any ideas, methods, instructions or products referred to in the content.